



**FACULTY
OF MATHEMATICS
AND PHYSICS**
Charles University

Summary of doctoral thesis

Dana Křížová

The source process of Greek earthquakes

Department of Geophysics

Supervisor of the doctoral thesis: Prof. RNDr. Jiří Zahradník DrSc.

Study programme: Physics

Specialization: Geophysics

Prague 2017



**MATEMATICKO-FYZIKÁLNÍ
FAKULTA**
Univerzita Karlova

Autoreferát dizertační práce

Dana Křížová

Ohniskový proces řeckých zemětřesení

Katedra geofyziky

Vedoucí dizertační práce: Prof. RNDr. Jiří Zahradník DrSc.

Studijní program: Fyzika

Studijní obor: Geofyzika

Praha 2017

Dizertace byla vypracována na základě výsledků získaných v letech 2008-2017 během doktorandského studia na Katedře geofyziky MFF UK.

Dizertant:

RNDr. Dana Křížová
Katedra geofyziky MFF UK
V Holešovičkách 2, 180 00 Praha 8

Školitel:

Prof. RNDr. Jiří Zahradník DrSc.
Katedra geofyziky MFF UK
V Holešovičkách 2, 180 00 Praha 8

Oponenti:

RNDr. Jiří Málek, Ph. D.
Ústav struktury a mechaniky hornin Akademie věd ČR, v.v.i.
V Holešovičkách 41, 182 09 Praha 8

RNDr. Jan Šílený, CSc.
Geofyzikální ústav Akademie věd ČR, v.v.i.
Boční II/1401, 141 31 Praha 4

Předsedkyně oborové rady:

Doc. RNDr. Hana Čížková, Ph. D.
Katedra geofyziky MFF UK
V Holešovičkách 2, 180 00 Praha 8

Autoreferát byl rozeslán dne

Obhajoba dizertace se koná dne 13. 9. 2017 v 10:00 hodin před komisí pro obhajoby dizertačních prací v oboru Geofyzika v budově MFF UK, Ke Karlovu 3, Praha 2, v místnosti M252.

S dizertací je možno se seznámit v PGS MFF UK, Ke Karlovu 3, Praha 2.

Contents

Introduction	1
1. Standard earthquake parameters and basic equations	2
1.1. Standard earthquake parameters	2
1.2. Essentials for calculations	3
2. Basic information for chosen earthquakes	6
2.1. Main information about selected areas in Greece	6
2.2. Crustal models for Greece, seismic stations and insight to moment tensor inversion	7
2.3. Santorini Island earthquakes	9
2.4. Cretan Sea earthquake	11
2.5. Synthetic tests	12
3. Accuracy of results	13
3.1. Moment tensor inversion – rating	14
3.2. Appraisal of results	19
3.3. Summary of Chapter 3	23
Conclusions	24
Bibliography	26
List of author’s publications and citation report	29

Introduction

Studies of the earthquake source process belong to seismologic priorities because of their relations to seismotectonics and simulations of strong ground motions. The earthquake source investigations have been performed at the Department of Geophysics (Faculty Mathematics and Physics, Charles University) since 90’s, most intensively in relation to seismic stations of the Faculty operating in Greece (since 1997) in cooperation with the University of Patras.

Although the location of earthquakes is common since the beginning of twentieth century, the moment tensor (MT) analysis starts much later, in 60’s (Aki and Richards, 2002; Lay and Wallace, 1995). Study of MT on regional distances is more complicated than computation with teleseismic data because of heterogeneities in the crust and the upper mantle. The most challenging source parameters are non-double-couple MT components, because their inversion is inherently least stable.

The present work links data processing and computational modeling to study source parameters of three carefully selected events in Greece: The Cretan Sea, M_w 5.3 event of 27 January 2012, the Santorini M_w 4.9 event of 26 June 2009, and the Santorini M_w 4.7 event of 26 June 2009. Their importance is in possible presence of the isotropic source component. The work focuses on methodical aspects of their centroid moment tensor (CMT) retrieval and its uncertainty. The main tool for this study is ISOLA software and its modifications. This package makes it possible to

compute moment tensors from regional and local full-waveform data for simple or multiple earthquakes. The method is being developed since 2003 (Sokos and Zahradnik, 2008).

Basic earthquake source parameters and equations, dealt with in this thesis, are listed in Chapter 1. Special attention is paid to moment tensor and their non-double-couple components. A detailed overview of the current state-of-art of the CMT determination and uncertainty assessment is given in Chapter 2, where the three earthquakes are introduced and analyzed. Chapter 3 describes the two main methodical innovations of the thesis:

(1) We investigate on synthetic tests and real data how to resolve the isotropic component of the seismic moment tensor, and how to evaluate its uncertainty. In the non-linear inversion problems, where there are eight free parameters (e.g., six elements of the moment tensor, depth, and origin time), we propose a waveform-inversion scheme in which the moment-tensor trace is systematically varied, and the remaining seven free parameters are optimized for each specific value of the trace.

(2) We propose a simple procedure to identify earthquakes with a strong isotropic component. The method consists of a comparison of the correlation-depth dependences for two modes of the CMT inversion: full and deviatoric.

The results have been summarized in two published papers (Křížová et al., 2013, and 2016).

1. Standard earthquake parameters and basic equations

We focus especially on solution of moment tensor inversion. We pay attention to earthquake kinematics. So, the earthquake dynamics is beyond the scope of this thesis.

1.1. Standard earthquake parameters

We chose six essential earthquake parameters which are commonly mentioned in earthquake reports (for example in web pages: European-Meditertanean Seismological Centre = EMSC or in Observatories & Research Facilities for European Seismology = Orfeus): origin time, depth, epicenter position, moment tensor, scalar seismic moment, magnitude.

Currently in seismology, the **moment tensor** – symmetric 3x3 tensor (MT) – is a common parameter of earthquakes and it is routinely used in everyday practice. Let us focus on centroid moment tensor in this work, because we calculate our solutions as a representation of major slip, not in hypocenter where the rupture propagation starts.

Moment tensor could be written in many types of coordinate systems. Most common are local geographic coordinate system (NED) i.e. the Cartesian system where the first coordinate x is positive from south to north, second y is positive from west to east and the last z downward.

The full MT could be decomposed – mathematically unique – into its deviatoric (DEV) and isotropic = volumetric (ISO = VOL) part:

$$\mathbf{M} = \mathbf{M}_{\text{DEV}} + \mathbf{M}_{\text{ISO}}. \quad (1.1)$$

DEV part can be further decomposed. Variety of schemes exist there (Jost and Herrmann, 1989; Julian et al., 1998). Usually \mathbf{M}_{DEV} is decomposed as follows:

$$\mathbf{M}_{\text{DEV}} = \mathbf{M}_{\text{DC}} + \mathbf{M}_{\text{CLVD}}, \quad (1.2)$$

where DC stands for largest possible double couple and CLVD is remainder component, the so-called compensated linear vector dipole. CLVD together with ISO represents non-DC part of MT.

If we invert waveforms corresponding to this \mathbf{M} under the assumption that the MT is purely deviatoric, we obtain $\mathbf{M}' = \mathbf{M}'_{\text{CLVD}} + \mathbf{M}'_{\text{DC}}$. It is obvious that, in general, $\mathbf{M}'_{\text{CLVD}}$ does not equal $\mathbf{M}_{\text{ISO}} + \mathbf{M}_{\text{CLVD}}$; therefore, \mathbf{M}'_{DC} does not equal \mathbf{M}_{DC} . Thus, we get a biased estimate of the DC%.

As Tape (2016) wrote, there are three different basic conventions for ISO, DC, and CLVD: Dreger et al. (2000), Vavryčuk (2001), and Chapman and Leaney (2012). We commonly use MT decomposition described in Vavryčuk (2001).

The most stable part of MT is DC, and this stability could persist even if there is noise in data or when the crustal structure is not well known (Jechumtálová and Šílený, 1998, 2001).

Scalar seismic moment M_0 is defined (Silver and Jordan, 1982) as:

$$M_0 = \sqrt{\frac{\sum_{p=1}^3 \sum_{q=1}^3 (M_{pq})^2}{2}}. \quad (1.3)$$

Basically this is the Euclidian norm of the MT.

The **magnitude** (M) represents relative size of an earthquake. This concept was proposed by Richter (1935). In this work, we use only moment magnitude M_w which is calculated from the scalar moment M_0 (in Nm).

$$M_w = \frac{2}{3} \log(M_0) - 6.06 \quad (1.4)$$

1.2. Essentials for calculations

In this thesis, we focus on shallow earthquakes particularly on events in the crust. So, we used regional records and all calculations were made in Cartesian geometry.

The MT is main result for us and its resolvability depends on conditionality of normal equations system in least squares method. Calculations on real data as well as extensive synthetic tests were made.

The MT full waveform inversion was performed using ISOLA – from ISOLated Asperities – software (Sokos and Zahradník, 2008, 2013) and with its

modifications. Many other codes also exist, e.g., TDMT_INVC software package – from Time-Domain Moment Tensor INVerse Code – (Dreger, 2002) and Kiwi tolls (Heimann, 2011; Cesca et al., 2010).

Nowadays many **crustal models** are obtained from travel-time studies, including 3D tomography, from dispersion curves or borehole experiments. In ISOLA we use 1D layered structural model where we define number of layers, and in each layer: top depth of layer, constant velocity of P-waves and S-waves, density, quality factors for P-waves and S-waves.

All our data has three components (north-south = NS, east-west = EW, vertical = Z). From records, we use only components without disturbances and with good signal to noise ratio.

At first, we provide information about event like origin time, location, magnitude, time length of seismograms. Then we clarify these parameters during calculations. (So, the number of tested positions of source and approximate origin time must be defined before calculations.) We set coordinates of stations and their names that we use during inversion.

According to Dahlen and Tromp (1998) or Aki and Richards (2002) we consider a **point source** of seismic waves of a given position and origin time:

$$u_i(t) = \sum_{p=1}^3 \sum_{q=1}^3 M_{pq} * G_{ip,q}, \quad (1.5)$$

where displacement \mathbf{u} is expressed by means of MT \mathbf{M} and spatial derivatives of Green's tensor \mathbf{G} ; * stands for temporal convolution and comma represents space derivative, p and q denote three Cartesian coordinates. The NED coordinate system was used in this work.

For solving linear partial differential equations, we use **Green's functions** (Green, 1828). Basically, it is impulse response of source in inhomogeneous media. As described in Aki and Richards (2002), Green's function is second degree tensor and depends on both receiver and source coordinates:

$$\rho \frac{\partial^2}{\partial t^2} G_{in} = \delta_{in} \delta(x - \xi) \delta(t - \tau) + \frac{\partial}{\partial x_j} \left(c_{ijkl} \frac{\partial}{\partial x_l} G_{kn} \right), \quad (1.6)$$

where unit impulse is applied at $\mathbf{x} = \xi$ and $t = \tau$ in the n -direction, than we denote the i th component of displacement at general (\mathbf{x}, t) by $G_{in}(\mathbf{x}, t; \xi, \tau)$.

The MT is symmetric and it can be expressed in the form of a linear combination of six **elementary** (dimensionless) **moment tensors** \mathbf{M}^i :

$$M_{pq} = \sum_{i=1}^6 a_i M_{pq}^i. \quad (1.7)$$

It represents a convenient parametrization because in this way the source is characterized by six scalar coefficients a_i .

These elementary tensors are implemented in the discrete-wavenumber code AXITRA (Bouchon, 1981; Countant, 1989). The other methodic aspects are similar like in Kikuchi and Kanamori (1991), but elementary MTs in that article differ from ours.

$$\begin{aligned}
M^1 &= \begin{pmatrix} 0 & 1 & 0 \\ 1 & 0 & 0 \\ 0 & 0 & 0 \end{pmatrix} & M^2 &= \begin{pmatrix} 0 & 0 & 1 \\ 0 & 0 & 0 \\ 1 & 0 & 0 \end{pmatrix} & M^3 &= \begin{pmatrix} 0 & 0 & 0 \\ 0 & 0 & -1 \\ 0 & -1 & 0 \end{pmatrix} \\
M^4 &= \begin{pmatrix} -1 & 0 & 0 \\ 0 & 0 & 0 \\ 0 & 0 & 1 \end{pmatrix} & M^5 &= \begin{pmatrix} 0 & 0 & 0 \\ 0 & -1 & 0 \\ 0 & 0 & 1 \end{pmatrix} & M^6 &= \begin{pmatrix} 1 & 0 & 0 \\ 0 & 1 & 0 \\ 0 & 0 & 1 \end{pmatrix}.
\end{aligned} \tag{1.8}$$

The $\mathbf{M}^1 - \mathbf{M}^5$ tensors represent five DC focal mechanisms, whereas \mathbf{M}^6 is purely ISO source. The six elementary tensors used here to aid the MT inversion should not be confused with various tensors used to decompose the MT for purposes of its physical interpretation, for example, to decompose into the isotropic part and three DC tensors (e.g., Julian, 1998, Jost and Herrmann, 1989).

The a -coefficients in equation (1.7) are related to \mathbf{M} as:

$$M = \begin{pmatrix} -a_4 + a_6 & a_1 & a_2 \\ a_1 & -a_5 + a_6 & -a_3 \\ a_2 & -a_3 & a_4 + a_5 + a_6 \end{pmatrix}. \tag{1.9}$$

The moment trace is related with just a single a -coefficient:

$$a_6 = \frac{\text{tr}(M)}{3}. \tag{1.10}$$

Moment tensor inversion belongs to the standard inverse problems. Theory of inverse problems is well described in Tarantola (2005).

Combining (1.5) and (1.7) we get

$$u_i(t) = \sum_p \sum_q \left(\sum_{j=1}^6 a_j M_{pq}^j \right) * G_{ip,q}, \tag{1.11}$$

and then

$$u_i(t) = \sum_j a_j \left(\sum_p \sum_q M_{pq}^j * G_{ip,q} \right) = \sum_{j=1}^6 a_j E_i^j(t), \tag{1.12}$$

where \mathbf{E}^j denotes the j th elementary seismogram corresponding to the j th elementary moment tensor and \mathbf{G} is Green's tensor.

If displacement \mathbf{u} and elementary seismograms are known, then inverse problem for a -coefficients can be solved. That is formally overdetermined problem because number of data (u_i) is much greater than number of parameters (a_j).

Here we assume that the moment temporal function is known, and it has the form of a step function, which is a good approximation at frequencies below the corner frequency of the event. In matrix notation

$$\mathbf{u} = \mathbf{E} \mathbf{a}. \tag{1.13}$$

This linear inverse problem for \mathbf{a} can be solved by the least-squares method. That could be written like system of equations

$$\mathbf{E}^T \mathbf{u} = \mathbf{E}^T \mathbf{E} \mathbf{a}, \tag{1.14}$$

with solution

$$\mathbf{a}_{\text{opt}} = (\mathbf{E}^T \mathbf{E})^{-1} \mathbf{E}^T \mathbf{u}, \quad (1.15)$$

where superscripts T and -1 stand for matrix transposition and inversion, respectively.

If the centroid position and time belong to the unknown parameters, they are sought through a spatiotemporal grid search in vicinity of a previously estimated position, and (together with \mathbf{M}) they collectively represent the CMT (centroid moment tensor) solution. In other words, we still solve linear problem (1.13) for \mathbf{a} but do so repeatedly with different \mathbf{E} .

The grid search maximizes the correlation between the observed (\mathbf{u}) and synthetic (\mathbf{s}) seismograms

$$Corr = \frac{\int us}{\sqrt{\int u^2 s^2}}, \quad (1.16)$$

where

$$\int us = \sum_i \int u_i(t) s_i(t) dt \quad (1.17)$$

and summation is over components and stations.

The match between real and best-fitting seismograms is measured by the L2-norm misfit

$$misfit = \int (u - s)^2 \quad (1.18)$$

and/or by means of the global variance reduction (VR):

$$VR = 1 - \frac{misfit}{\int u^2} = 1 - \frac{\int (u - s)^2}{\int u^2} = Corr^2. \quad (1.19)$$

Let us mention the fact that if synthetics s are found by the least-squares misfit minimization of $\int (u-s)^2$, then $\int us = \int ss$ (see, e.g., equations 1-6 of Kikuchi and Kanamori, 1991). That is why VR and correlation are simply related by (1.19).

2. Basic information for chosen earthquakes

2.1. Main information about selected areas in Greece

Greece is in general one of the most seismically active areas in Europe. It is divided into 13 regions plus there is one autonomous area. We would like to focus on two of them: Crete and South Aegean. From the past, we could mention our interest in Movri Mountain earthquake in Western Greece region (Galovič et al., 2009).

Our areas of interest are shallow earthquakes with possible nonzero isotropic component. We focused on south-central Aegean region not far from Columbo volcano. The tectonic settings and stress field characteristics of this area are well described and depicted in Karagianni et al. (2005).

A moderate earthquake swarm started on 26 June 2009 northeast of the Santorini (Thira) Island, close to Mt. Columbo, an active submarine volcano in the

Cyclades, Aegean Sea. The swarm occurred at the western boundary of the Santorini–Amorgos zone, a major structural unit in the Hellenic volcanic arc.

We investigate also shallow event of the south-central Aegean region: the 27 January 2012 M_w 5.3 Cretan Sea earthquake, the strongest event of the January 2012 earthquake sequence in Cretan Sea.

Broadband waveforms were retrieved from the permanent stations of the Hellenic Unified Seismic Network (HUSN), operated jointly by the National Observatory of Athens (NOA, doi:10.7914/SN/HL), the Aristotle University of Thessaloniki (AUTH, doi:10.7914/SN/HT), the University of Patras (UPSL, doi:10.7914/SN/HP), and the University of Athens (UOA). The records from one station of the National Seismic Network of Turkey (DDA) were also used. A few UPSL stations are co-operated by the Charles University.

The selection of the events is motivated by the following:

1. events were well recorded by broadband instruments of a reasonable azimuthal coverage;
2. they occurred at a region where tectonic and volcanic events can occur, making them candidates for possibly large ISO components;
3. the previous analyses have revealed that the events may have a quite different ISO content, in particular a large ISO during the strongest event of Santorini earthquake swarm.

Although we basically focus on synthetics tests, we start with real data because in the synthetics tests we will use the same source-station configuration.

2.2. Crustal models for Greece, seismic stations and insight to moment tensor inversion

Crustal velocity models for Greece

The most common models for Greece are i.e., Haslinger et al. (1999), Latorre et al. (2004), Rigo et al. (1996), and Karagianni et al. (2005). Model “M1” (Tselentis et al, 1996) is occasionally used for locations. 1-D regional crustal models Novotný et al. (2001), and Dimitriadis et al. (2010) were used for moment tensor inversion in this thesis. These two models are depicted in the Figure 2.1. The model by Novotný et al. (2001) was obtained from the regional surface-wave dispersion, in which Lg waves dominate, and it is routinely used for MT inversions at AUTH; and the model by Dimitriadis et al. (2010) based on local first-arrival times.

Seismic stations used

Twenty stations were used during calculations. Their position is shown in the Figure 2.2. The records from the broadband seismographs are used, so, instrumental corrections of data were made. Stations Nisiros Isl. and Nisiros are on the same island, so, they are shown very close one to the other in the map.

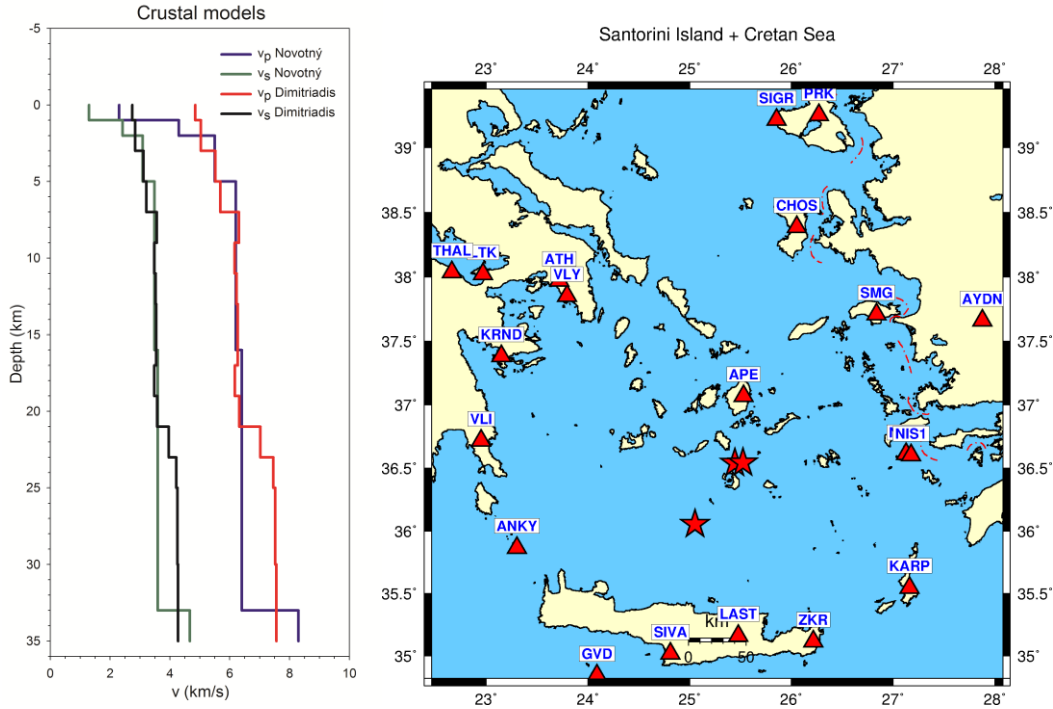


Figure 2.1. (left) 1-D Crustal models Novotný et al. (2001) and Dimitriadis et al. (2010) used in inversion.

Figure 2.2. (right) Broadband seismic stations (triangles) used in calculations for papers Křížová et al. (2013) and Křížová et al. (2016). Epicenters for selected events are marked with asterisks.

Insight to moment tensor inversion

The MT inversion was performed using ISOLA software (Sokos and Zahradník, 2008). ISOLA is a program package based on the multiple point-source iterative deconvolution of complete regional waveforms. This is based on method from Kikuchi and Kanamori (1991). Green's functions are calculated by the discrete-wavenumber method (Bouchon, 1981; AXITRA code of Coutant, 1989). The moment tensor is solved by the least-squares method, and the origin time and 3D position of the point source (centroid) are both grid-searched, the latter in the vicinity of the (independently) located hypocenter. The correlation between real = observed and synthetic seismograms – eq. 1.16 – is maximized. In the preliminary stage, we considered variations of the centroid position both in the horizontal direction and depth. In the following discussions, for simplicity, we concentrate only on grid searching the centroid depth (Křížová et al., 2013; 2016). The method is routinely used in the Seismological Laboratory of the University of Patras to calculate moment tensors in western Greece. Currently ISOLA became one of standard software for MT calculation and it is widely used (i.e., Hicks and Rietbrock, 2015). Here we use a single point-source approximation. Each event is characterized by its strike, dip, rake, centroid depth, scalar moment M_0 , moment magnitude M_w , the percentages of ISO, DC, and abs(CLVD), the global VR.

2.3. Santorini Island earthquakes

We investigate two strongest events ($M_w > 4$) of moderate earthquake swarm which started on 26 June 2009 close to an active submarine volcano in Aegean Sea. The sequence was rich in earthquakes, with about 25 events with M_w larger than 2.5 within the first five days. The earthquakes were recorded with a good azimuthal coverage at epicentral distances approximately from 60 to 310 km. We use the records from 15 and 10 stations of events 1 and 2, respectively. The seismograms which provided a good signal-to-noise ratio even at relatively low frequencies (0.02-0.1 Hz) were chosen.

The stability of the MT solution was further examined by jackknifing the data (i.e., systematically removing one station from the inverted data set). *Event 1 has a relatively large ISO percentage in model N. Event 2 is characterized by the opposite sign of ISO in the two applied crustal models.*

As has been said, all calculations were provided in two crustal models: model N - Novotný et al. (2001) and model D - Dimitriadis et al. (2010). Full MT, deviatoric MT, and DC-constrained MT were calculated. Basic information and results are summarized in the Table 3 and in the Figure 2 in Křížová et al. (2013).

The most remarkable difference between the full-MT solutions of event 1 is due to the crustal models used, especially in the case of the 10 stations, where the explosion-like mechanism in model N changes to implosion in model D. The latter has a greater variance reduction. Another important feature is the different centroid depth of the deviatoric and full-MT solutions, while their variance reductions are almost the same. It indicates the trade-off between the depth and the non-DC part of the MT.

Strongest event – Santorini earthquake

We made calculations with records from all 15 available stations (ordered from the closest to the most distant, they are: APE – LAST – NIS1 – ZKR – SIVA – KARP – ANKY – CHOS – ATH – VLI – AYDN – LTK – THAL – SIGR – PRK) and also using only 10 stations which are accessible for weaker event (the second strongest Santorini Island earthquake). This earthquake M_w 4.9 occurred 26 June 2009 at 20:37:38.10 UTC and it was located in the depth 9.7 km at position: 36.531°N; 25.434°E.

Some station components were excluded due to low signal to noise ratio. In the first step, we search MT solution under epicenter (located by the Aristotle University of Thessaloniki, Department of Geophysics) with the depth step 0.5 km. Then we try to find better solution in the area close to previous result, so, 3D grid search was made. Then we use coordinates from new centroid position for further calculations. The results for specified position are in Table 3 in Křížová et al. (2013) where new centroid position for model N is: 36.5400 °N; 25.4452°E, and for model D is: 36.5490 °N; 25.4563 °E. For simplicity, and to avoid misinterpretation in synthetic tests (especially in the test C) of Křížová et al. (2016), only one geographical position – same as for model N in previous article – was used during

the calculations. The results for deviatoric MT and full MT calculations below epicenter are summarized in the Table 2.1. and in the Figure 2.3. Note that results mentioned in the Table 3 in Křížová et al. (2013) and in the Table 3 in Křížová et al. (2016) slightly differ from each other because in the first case we use depth step 0.5 km during calculations and 1.0 km in the second case.

Table 2.1.: Solution for MT inversion for strongest event of Santorini Island earthquake swarm

	Model N			Model D								
	Full MT			Dev. MT								
strike; dip; rake (°)	252	68	-59	240	62	-78	248	66	-63	244	65	-76
	13	36	-142	36	29	-111	16	35	-136	34	28	-117
M_w	4.7			4.6			4.7			4.7		
M_0 (Nm)	1.146 x 10 ¹⁶			9.931 x 10 ¹⁵			1.328 x 10 ¹⁶			1.192 x 10 ¹⁶		
depth (km)	6.5			3.5			6.0			2.5		
Centroid time (s)	20: 37: 37.65			20: 37: 37.65			20: 37: 39.15			20: 37: 39.15		
DC	28.3			70.5			36.1			69.0		
CLVD	16.6			29.5			10.5			31.0		
ISO	55.1			0.0			53.4			0.0		
VR	0.65			0.64			0.68			0.68		

Dev. ... Deviatoric; M_0 ... scalar seismic moment (eq. 1.4); M_w ... magnitude (eq. 1.5)

VR ... variance reduction (eq. 1.20)

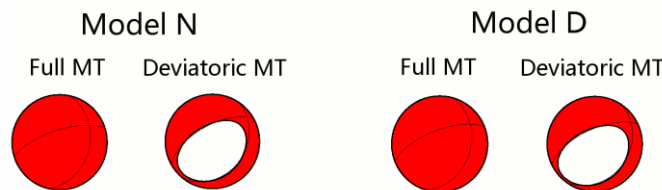


Figure 2.3. MT solutions for strongest event of Santorini Island earthquake swarm.

Weaker event – Santorini earthquake

The second strongest earthquake M_w 4.7 from the swarm occurred 26 June 2009 at 22:14:53.50 UTC, and it was located in the depth 4.1 km at position: 36.544 °N; 25.523°E. Results of MT inversions are summarized in the Table 3 in Křížová et al. (2013).

We made calculations with records from 10 stations (APE – LAST – ZKR – KARP – CHOS – ATH – VLI – LTK – SIGR – PRK). Some station components were excluded due to low signal to noise ratio.

As same as for the strongest event of the swarm, in the first step, we search MT solution under epicenter with the depth step 0.5 km, followed by a 3D grid search. Then we use coordinates from new centroid position for further calculations.

The results for specified position are in Table 3 in Křížová et al. (2013) where new position for both model N and D is: 36.5440 °N; 25.4668°E. The results for deviatoric MT and full MT calculations below epicenter are summarized in the Table 2.2 and in the Figure 2.4.

Table 2.2.: Solution for MT inversion for the second strongest event of Santorini Island earthquake swarm

	Model N			Model D		
	Full MT		Dev. MT	Full MT		Dev. MT
strike; dip; rake (°)	265 55 -40	257 50 -57	244 45 -71	244 45 -70	21 57 -137	31 49 -123
M_w	4.4	4.4	4.5	4.5	28 47 -108	37 47 -108
M_0 (Nm)	4.467×10^{15}	4.051×10^{15}	5.600×10^{15}	5.327×10^{15}		
depth (km)	6.5	4.5	4.0	4.5		
Centroid time (s)	22: 14: 52.80	22: 14: 52.80	22: 14: 53.80	22: 14: 53.75		
DC	40.5	75.7	78.7	80.4		
CLVD	26.6	24.3	9.6	19.6		
ISO	32.9	0.0	-11.8	0.0		
VR	0.62	0.61	0.65	0.66		

Dev. ... Deviatoric; M_0 ... scalar seismic moment (eq. 1.4); M_w ... magnitude (eq. 1.5)
VR ... variance reduction (eq. 1.20)

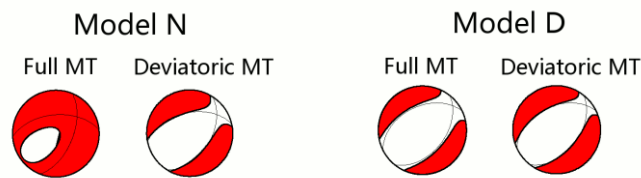


Figure 2.4. MT solutions for the second strongest event of Santorini Island earthquake swarm.

2.4. Cretan Sea earthquake

The earthquake sequence occurred in southwest direction from Santorini Island. The Cretan Sea earthquake is the strongest event of the January 2012 earthquake sequence in Cretan Sea. For this earthquake only crustal model Novotný was used, because hypocenter of this event is in the slightly different place than in case of Santorini Island events and model Dimitriadis seems to be inappropriate.

This earthquake M_w 5.3 occurred 27 January 2012 at 01:33:24.0 UTC and it was located in the depth 10 km at position: 36.044°N; 25.064°E.

We made calculations with records from 12 stations. All station components have quite good signal to noise ratio. In order from closest to furthermore they are: SIVA - APE - ZKR - ANKY - GVD - NISR - KARP - VLI - KRND - VLY - SMG - CHOS.

As same as for the Santorini earthquakes, in the first step, we search MT solution under epicenter, but in this case the depth step 1 km was used. Then we try to find better solution in the area close to previous result, so, 3D grid search was made. Then we use coordinates from new centroid position for further calculations.

The results for specified position are in Table 2 in Křížová et al. (2016) where new position is: 36.056 °N; 25.053°E. The results for deviatoric MT and full MT calculations below epicenter are summarized in the Table 2.3 and in the Figure 2.5.

The stability of the MT solution was further examined by jackknifing the data.

Table 2.3.: Solution for MT inversion for the strongest event of Cretan Sea earthquake swarm

	Full MT	Dev. MT
strike; dip; rake (°)	182 84 -110	187 84 -110
	82 21 -16	81 21 -16
M_w	5.4	5.4
M_0 (Nm)	1.247×10^{17}	1.245×10^{17}
depth (km)	7.	7.
Centroid time (s)	01: 33:24.5	01: 33: 24.5
DC	84.3	89.4
CLVD	10.1	10.6
ISO	-5.6	0.0
VR	0.63	0.63

Dev. ... Deviatoric
 M_0 ... scalar seismic moment (eq. 1.4)
 M_w ... magnitude (eq. 1.5)
 VR ... variance reduction (eq. 1.20)

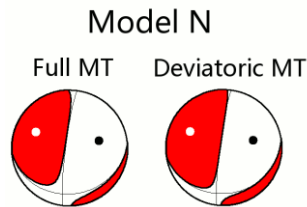


Figure 2.5. MT solutions for the strongest event of Cretan Sea earthquake swarm.

2.5. Synthetic tests

For synthetic tests, we will use the same source-station configuration as for two shallow events of the south-central Aegean region: the 27 January 2012 M_w 5.3 Cretan Sea earthquake and the 26 June 2009 M_w 4.9 Santorini earthquake.

Motivation of the synthetic tests comes from observatory practice. Besides the centroid position and the strike/dip/rake angles, we are often interested in the DC% because this is the simplest parameter characterizing a possible deviation of the earthquake from pure shear faulting. We seek to understand how the obtained DC% depends on the adopted MT-inversion mode.

All tests have a common feature. We calculate synthetic waveforms for an assumed centroid position and for a given full MT. We then invert the synthetic waveforms in either a full-MT or deviatoric-MT mode and we leave the centroid depth and time free. We investigate the effects of the deviatoric constraint on the obtained source parameters (strike/dip/rake, depth, DC%, etc.). Three tests are made (A–C), each one with six subtests (1-6). For simplicity, all models have CLVD% = 0.

Technically, the subtests are created as follows: we choose the strike/dip/rake angles and calculate the a -coefficients (eq. 1.9) a_1, \dots, a_5 , of the deviatoric MT. Then, we create full MTs of several ISO components by choosing appropriate values of the sixth coefficient a_6 .

The MT-inversion results for synthetic tests A-C including the subtests 1-6 are mentioned in corresponding Tables A3–A5 of Křížová et al. (2016). Several interesting features are discussed in this article mentioned above.

Test A corresponds to Cretan Sea earthquake. It means the centroid depth and strike/dip/rake angles are same as in real case for full MT (see Table 2 in Křížová et al., 2016). The true depth for this test is 8 km. The subtests differ in their ISO% (rounded to integer values): ± 90 , ± 46 , and ± 30 . The plus and minus signs correspond to explosion and implosion, respectively. Synthetic data are forward simulated and inverted using the same velocity model (N-model).

Test B corresponds to Santorini earthquake (the strongest event from swarm). It means the centroid depth and strike/dip/rake angles are same as in real case for full MT in model N (see Table 3 in Křížová et al., 2016). The true depth for this test is 6 km. The subtests differ in their ISO% (rounded to integer values): ± 90 , ± 48 , and ± 32 . Synthetic data are forward simulated and inverted using the same velocity model (N-model).

Test C corresponds to Santorini earthquake (the strongest event from swarm). It means the centroid depth and strike/dip/rake angles are same as in real case for full MT in model N (see Table 3 in Křížová et al., 2016). The true depth for this test is 6 km. The subtests differ in their ISO% (rounded to integer values): ± 90 , ± 48 , and ± 32 . Test C is more complicated than previous two tests. To illustrate possible effects of inaccurate velocity models, we forward simulate synthetic waveforms in one model (N-model), but invert them in the other (D-model). That is why in Test C, variance reduction (eq. 1.19) is always less than 85%. We could also see difference between “real” ISO values and values obtained from MT calculations (-90 vs -70 ; $+90$ vs $+75$; ± 48 vs ± 50 ; ± 32 vs ± 34).

3. Accuracy of results

The analysis of resolvability and uncertainty of the MT belongs to main part of modern seismology. The focal mechanism (i.e. the strike, dip, rake and scalar moment) is relatively stable with respect to inaccuracies of the routinely available velocity models and also with respect to possible errors in the assumed source positions. Nevertheless, to make the focal mechanism even more reliable, the source (centroid) position and time are in our case jointly inverted with the mechanism. Contrarily to the focal mechanism, the non-DC components of MT (CLVD and ISO) are difficult to determine because they are unstable. It means that they vary a lot with small changes of the velocity model, source-station configuration, and frequency range, among others.

We would like to answer the question if it is necessary always calculate full MT instead of deviatoric MT, while we know that only its strike/dip/rake (and moment) are reliable. Is the percentage of the DC part (hereafter, DC%) well determined if derived from the deviatoric MT? We would like to analyze how the

deviatoric constraint affects the MT inversion results such as the DC%, the centroid depth, and the strike/dip/rake angles.

3.1. Moment tensor inversion - rating

There exist many methods how to analyze results of MT inversion. Before to concentrate on comparing outcomes we should mention how we try to avoid wrong evaluation of calculations.

In the first step, we select satisfactory data with good signal to noise ratio and without disturbances. Then we try to find a suitable frequency range for full waveform inversion. In this thesis, we used band pass filtering defined by four frequencies, it means that the filter has two cosine tapered windows, one on each side, and in the inner interval the filter is constant. For both Santorini events, it is 0.02 – 0.05 – 0.08 – 0.1 Hz and for Cretan Sea earthquake it is 0.03 – 0.05 – 0.08 – 0.1 Hz. It is worth mentioning that this filter is non-causal. Currently, a causal Butterworth filter has been implemented into ISOLA software, which is defined only with two corner frequencies. In both cases (causal or non-causal) the same filter is applied to real and synthetic data. The main uncertainties became from insufficient knowledge of the Greens function, which means crustal model and seismic source position. To reduce crustal model uncertainty, we are trying to use as longest periods as possible.

Conventional methods – results comparison

Correlation and variance reduction

As stated in Chapter 2, we try to maximize correlation between the observed (u) and synthetic (s) seismograms (eq. 1.16). We suppose that the moment rate function is a delta function, which is a good approximation at frequencies below the corner frequency of the event. Then eq. (1.12) can be understood as a linear inverse problem for unknown a 's, hence, the unknown moment tensor \mathbf{M} . The full MT inversion seeks all six a 's, while the deviatoric inversion (DEV) assumes $a_6=0$, therefore only the first five a 's are calculated. The synthetic seismograms (s) are in inverse problem searched by the least-squares misfit minimization. Like an optimal source depth (position) and origin time are considered results for which the shape match between observed and synthetic seismograms is the best. The main tool to evaluate results is then correlation and variance reduction (eq. 1.19).

Correlation diagrams

The correlation between observed and synthetic data is depicted as a function of position, which at the same time show appropriate source mechanism for all tested positions. At each position, we plot the best result from the temporal grid search.

Here we analyze whether there is any simple feature in these complex results, at least for some specific values of ISO%. Therefore, we further concentrate on the variation of the waveform correlation with trial source depth, and we will show that

indeed the events with a large ISO% may have a specific correlation-depth behavior. As an example, see Figures 7 and 8 of Křížová et al. (2016).

Kagan angle

To measure the angular departure of any two DC solutions, under comparison, we use Kagan angle (Kagan, 1991). The solutions are comparable (quite similar) if the angle is $< 10^\circ$ - 20° , and highly dissimilar if the angle is $> 40^\circ$.

Let us mention that full MT and deviatoric MT for first subtest B are enormously different (Kagan angle = 88°), also full MT in model D in the second subtest C differ a lot from right solution (Kagan angle = 91°).

Condition number

To examine how well or ill posed the inverse problem is we additionally use the condition number CN. The condition number (CN), is defined by

$$CN = \frac{\max_{i=1,\dots,6} (w_i)}{\min_{i=1,\dots,6} (w_i)}. \quad (3.1)$$

Here w denotes the singular numbers of the matrix of elementary seismograms. CN is useful in judging, at least in a relative sense, how well or ill posed is the inverse problem; small singular values (large CN) indicate an unstable solution. The w_i are expressed in eq. (3.6) below in this section.

The CN is a relative measure; a larger CN signalizes a worse (less stable) resolvability of MT. E.g. some cases of large CN for model D: CN = 16 for full MT inversion - strongest Santorini event for ten stations used during calculations, CN = 6 for full MT inversion - second strongest Santorini event.

Other standard methods for results evaluation

Like a standard stability tests the jackknife tests were performed. This means that we made calculations repeatedly and in each calculation one station was excluded from data set.

For comparison of moment tensors, we can use also another parameter, μ . According to Pasyanos et al. (1996):

$$\mu = \sqrt{\frac{\sum_{i=1}^3 \sum_{j=1}^3 \left(\frac{M_{1ij}}{M_{01}} - \frac{M_{2ij}}{M_{02}} \right)^2}{8}}, \quad (3.2)$$

where indices 1, 2 mark the first and the second result respectively. M_{ij} stands for components of MT and M_0 is scalar seismic moment (eq. 1.3). Values of μ range from 0. to 1., where 0. stands for identical solutions and for μ less than 0.25 the results are considered to be highly similar, and good agreement is for μ less than 0.35. In this thesis the Kagan angle is preferred instead of μ for solution comparison.

New approach for results assessment

Now, we would like to focus on isotropic component of MT. Prior to the application using observed data, we performed a number of tests to validate the approach.

Probability density function

First, we deal with the linear MT inversion with six parameters (a fixed centroid position and time) and present a theoretical 1D pdf allowing for the simplest estimate of the ISO uncertainty in the 6D parameter space (Zahradník and Custódio, 2012). Then we propose an extension into the nonlinear MT inversion in the 8D parameter space (i.e., the six-component MT, centroid depth, and time).

First, we assume that the centroid depth H and time O are known (fixed), the MT inverse problem has 6 parameters and is linear, and thus the uncertainty analysis is straightforward. Since $\text{tr}(\mathbf{M})/3 = a_6$ is one of the model parameters, we can analytically calculate its standard deviation σ_{a_6} . For theoretical reasons, we have to introduce a standard deviation σ_u of the data. Its squared value is the data variance. We assume the simplest possible case that σ_u has the same value for all the data components and is independent of time. It is not easy to estimate the true value of σ_u , however, in problems such as the one solved in this paper, where we investigate the uncertainty in a relative sense only, we just prescribe a reasonable value of σ_u , and keep it constant in all the compared models. Here by ‘reasonable value’ we mean σ_u of the same order of magnitude as the peak-to-peak amplitude of the displacement data in the studied frequency range at the most distant station, i.e. $\sigma_u = 1 \times 10^{-5}$ m.

In this section, we proceed according to Press et al. (1997). Normalizing \mathbf{u} and \mathbf{E} of Equation (1.14) by the standard deviation, we obtain

$$\tilde{u} = \frac{u}{\sigma_u}; \quad \tilde{E} = \frac{E}{\sigma_u}; \quad \tilde{u} = \tilde{E} a, \quad (3.3)$$

where \tilde{E} is the design matrix. The design matrix depends on the position of the source and stations, on the crustal model and the considered frequency range, but does not depend on the waveforms. We can assess the *theoretical* parameter uncertainty even without recorded seismograms. Any single parameter a_i then has a 1D Gaussian probability density function (pdf). For a_6 we have

$$pdf(a_6) = \frac{e^{-\frac{1}{2} \frac{(a_6 - a_{6opt})^2}{\sigma_{a_6}^2}}}{\sigma_{a_6} \cdot \sqrt{2\pi}}, \quad (3.4)$$

where the true value of a_6 is denoted a_{6opt} , and the standard deviation σ_{a_6} is given by the explicit formula (Press et al., 1997, section 15.4)

$$\sigma_{a_6}^2 = \sum_{i=1}^6 \left(\frac{V_{6i}}{w_i} \right)^2. \quad (3.5)$$

Here V_{6i} is the 6th component of the i -th singular vector of the design matrix \tilde{E} , and w_i is its i -th singular value. In practice, we do not need the singular decomposition of

matrix $\tilde{\mathbf{E}}$, since the singular vectors \mathbf{V} of $\tilde{\mathbf{E}}$ are simply eigenvectors of matrix $\mathbf{E}^T\mathbf{E}$, and the singular values of $\tilde{\mathbf{E}}$ can be calculated from the eigenvalues λ_i of $\mathbf{E}^T\mathbf{E}$:

$$w_i = \sqrt{\frac{\lambda_i}{\sigma_u^2}}, \quad i=1,2,\dots,6 \quad (3.6)$$

Now consider $\Delta\chi^2$, i.e. the theoretical misfit between data and synthetics, normalized by the data variance. The surfaces of constant theoretical misfit $\Delta\chi^2$ (a 6D ellipsoid) are given by (Press et al., 1997 section 15.6.)

$$\Delta\chi^2 = w_1^2(\mathbf{V}_{(1)} \cdot \delta\mathbf{a})^2 + \dots + w_6^2(\mathbf{V}_{(6)} \cdot \delta\mathbf{a})^2 \quad (3.7)$$

where $\delta\mathbf{a}$ is the radius vector connecting the center of the ellipsoid and a point in the parameter space. It enables us also to *numerically* study misfit as a function of $a_1 - a_6$, or its particular projection onto a single parameter axis (the a_6 -axis). Theoretical justification of the projected misfit and its relation to confidence intervals of the single parameter comes from section 15.6., Theorem D of Press et al. (1997). We discretize a_6 , and for each value of a_6 we extract the points inside the ellipsoid (a_1, a_2, \dots, a_5)| a_6 ; here | a_6 denotes a fixed value of a_6 . Each point is characterized by the theoretical misfit $\Delta\chi^2(a_6) \leq 1$, and we determine its minimum value $\Delta\chi^2_{\min}$ over all points (a_1, a_2, \dots, a_5)| a_6 . Then we define:

$$\textit{Theor_pdf}(a_6; H = \textit{fixed}; O = \textit{fixed}) = e^{-\frac{1}{2} \min_{\textit{theor_misfit}(a_1, \dots, a_5)} | a_6} \quad (3.8)$$

Here the minimum theoretical misfit $\Delta\chi^2_{\min}$ was denoted $\min_{\textit{theor_misfit}}$; note that a_6 is a free parameter that is varied, not computed by the inversion. Similar function was further used in a non-linear case. For consistency with the published paper, we use the term ‘‘1D probability density function’’ also here, making warning, that it is a formal quantity which should not be confused with the statistically justified marginal probability density function of a_6 .

In non-linear case, the inverse problem has 8 parameters: a_1, \dots, a_6, H , and O . The non-linearity is due to the effect of the centroid depth H and centroid time O . The theoretical misfit function is no longer available. Thus, we use waveforms and evaluate the real misfit between the data and synthetic seismograms, i.e. misfit eq. (1.19) normalized by the data variance. In analogy to eq. (3.8), the so-called *experimental* probability density function can be evaluated:

$$\textit{Exper_pdf}(a_6; H = \textit{free}; O = \textit{free}) = \textit{const} \cdot e^{-\frac{1}{2} \min_{\textit{real_misfit}(a_1, \dots, a_5, H, O)} | a_6} \quad (3.9)$$

Here the minimal real misfit is denoted $\min_{\textit{real_misfit}}$. The meaning of eq. (3.9) is as follows: A value of a_6 is chosen, and the real misfit is minimized by the least-squares method in a_1, \dots, a_5 , and by a grid search in H and O . Repeating this for a set of discrete a_6 values, we obtain a 1D pdf(a_6) reflecting the linear effect of a_1, \dots, a_5 and non-linear effects of H and O . The value of *const* normalizes the integral of pdf(a_6) to unity. The 1D experimental pdf in eq. (3.8) is the main new tool proposed in this study. *Although the proposed method yields a 1D pdf(a_6), it takes into account the 8D nature of the problem, as well as its nonlinearity. On the other hand, the*

uncertainty of the crustal structure model is not included. It must be solved by repeating the analysis using several models that are available.

Remark: Again, we emphasize that we study projection of 8D misfit onto one of the parameter axes (the a_6 -axis), not a marginal probability density of a_6 .

The only technical issue related to eq. (3.9) that requires caution is the minimization of the misfit for each fixed value of a_6 . For each a_6 we must find the optimal centroid depth H and time O common to all a_1, \dots, a_6 . The algorithm is the following: We choose a discrete value of a_6 , (close to the previously computed optimal value, but not equal to this value) and a given trial value of H and O . We minimize the misfit between real data \mathbf{u} and synthetics \mathbf{s} , thus obtaining a_1, \dots, a_5 . Combining these inverted coefficients with the chosen coefficient a_6 we obtain \mathbf{a}_{opt} . The correlation between \mathbf{u} and $\mathbf{s}=\mathbf{E} \mathbf{a}_{\text{opt}}$ is calculated using eq. (1.16). The procedure is repeated for each trial O and H (still fixing the same a_6), and the H and O with maximum correlation are found for the chosen value of a_6 . The whole procedure is repeated for each value of a_6 . As a result we obtain the best-fitting parameters (a_1, \dots, a_5, H, O), as well as the minimum misfit value (i.e. the *min real_misfit* value), all as a function of a_6 . Thus, we construct the desired experimental pdf(a_6) according to eq. (3.9).

Another way of obtaining probability density functions of various source parameters (including ISO) has been recently proposed by Vackář et al. (2017). At each trial depth and time the best-fitting MT tensor is calculated by the least-squares method, and the minimum misfit is converted into an exponential PDF (probability density function). The individual PDF's are used to provide Gaussian random MT samples whose number at each depth is determined by integrating PDF over the MT parameters. This procedure normalizes the complete (generally non-Gaussian) PDF to unity. Complete set of the MT samples (for all trial depths and times) enables construction of histograms (marginal PDF's) of the source parameters, including ISO.

Determination of depth during full MT and deviatoric MT inversions

The centroid position is commonly searched together with MT. We would like to answer the question if it is necessary to calculate full MT instead of deviatoric MT even if we are not interested in value of ISO. The synthetic tests were performed in Křížová et al. (2016) for this reason.

The inversion of the synthetic data in deviatoric mode in our case clearly shows that neglecting the isotropic component has a strong effect upon the correlation-depth variations. In particular, sub-tests with high ISO component (in absolute value) show very deep local minima, but weaker local minima can be observed also in the other sub-tests. The minima are close (but not identical) to the true source depth. This remarkable feature is common to all our tests. The tests indicate that if a real event has a very large ISO% (low DC%), the correlation-depth graph may get an apparent minimum near the correct source depth, i.e. the depth will be incorrectly determined.

The significantly different correlation-depth profiles can be simply explained. Imagine a source at depth D with a large ISO component and negligible CLVD. This ISO component constitutes a significant part of the waveforms. In the full-MT inversion the waveforms can be best fitted at the depth D . However, in the deviatoric-MT inversion the true waveforms are approximated with synthetics lacking the ISO part. It means that real data are interpreted in terms of an inappropriate model (DC and CLVD only), hence deteriorating the match at depth D . As the inappropriate model does not contain ISO, real data could be partially fit only by a source model at depth D having a different focal mechanism, biased with respect to the true one in a way compensating the missing ISO. However, if no biased deviatoric MT can compensate the lack of ISO, a correlation minimum is created. At another trial depth, $D' \neq D$, some deviatoric-MT source model can exist (for example, a model with a spurious CLVD, and/or with biased strike, dip, and rake angles) that produces synthetics fitting real data almost as well as the full-MT synthetics at depth D . Hence the source depth estimate in the deviatoric-MT inversion may be biased from D to D' .

3.2. Appraisal of results

Standard results obtained during calculations are mentioned in Křížová et al. (2013, 2016), so we do not repeat all results from articles and we focus only on some of them.

Santorini island - strongest event - results

In this section, we would like to compare results for eq. (3.9) with calculations according equations (5-7) of Vackář et al. (2017), recently implemented in ISOLA. Let us mention that in the first case (eq. 3.9) we use “old” ISOLA software with non-causal filter 0.02 – 0.05 – 0.08 – 0.1 Hz and in the second case (eqs. 5-7 in Vackář et al, 2017) the causal filter 0.04 – 0.1 Hz was used.

For this reason, let us start with summary of the results for standard full MT inversions, which are summarized in the Table 3.1 and shown in the Figure 3.1. We can see that results almost do not differ from each other for full MT inversion in model N and D respectively. The solutions for causal filter have larger variance reduction and smaller condition number. The main difference is in value of ISO component for model D. According to lower CN, we prefer the value 47.3 % obtained for inversion with causal filter. (Note that we obtain and introduce the DC, CLVD, and ISO values to one decimal place instead of rounded them to integers, but this is due to the fact that then is easier to put their sum equal to 100% correctly.)

The results for pdf function calculations according to eq. (3.9) and histograms corresponding to equations (5-7) of Vackář et al. (2017) are shown in the Figures 3.2 – 3.3. In the Figure 3.2 we can see that resolvability of ISO component is better if real velocity structure is closer to model N than D, and the same applies for histograms in the Figure 3.3. In this sense, the two methods are in rough agreement. Comparison of thesis methods is shown in the Figure 3.3 where a_6 from eq. (3.9) are

recalculated to ISO and maximum value of pdf function is formally adjusted on the same level as maximum in histogram.

Table 3.1.: Solution for full MT inversion for strongest event of Santorini Island earthquake swarm for using non-causal and causal filtration during calculations

	Model N			Model D								
	non-causal		causal	non-causal		causal						
strike; dip; rake (°)	255	69	-57	255	69	-57	253	65	-67	250	65	-63
	15	38	-144	16	37	-143	27	32	-130	20	35	-133
M_w	4.7			4.7			4.7			4.7		
M_0 (Nm)	1.124×10^{16}			1.126×10^{16}			1.167×10^{16}			1.224×10^{16}		
depth (km)	6.5			6.5			4.0			5.5		
Centroid time (s)	20: 37: 37.75			20: 37: 37.85			20: 37: 39.25			20: 37: 39.30		
DC	41.9			44.0			48.5			49.9		
CLVD	5.0			2.5			28.0			2.8		
ISO	53.1			53.5			23.5			47.3		
VR	0.66			0.70			0.70			0.73		
CN	3.34			3.06			5.09			3.10		

Dev. ... Deviatoric; M_0 ... scalar seismic moment (eq. 1.4); M_w ... magnitude (eq. 1.5)

VR ... variance reduction (eq. 1.20); CN ... condition number (eq. 3.1)

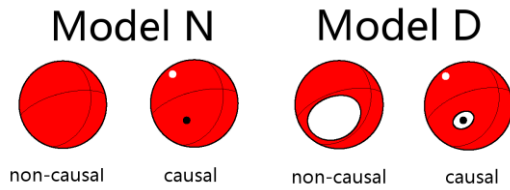


Figure 3.1. Full MT solutions for strongest event of Santorini Island earthquake swarm.

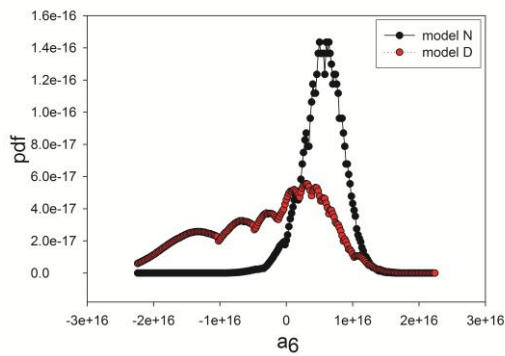


Figure 3.2. The uncertainty assessment of the isotropic component, $pdf(a_6)$, calculated using equation (3.9) in two crustal models, N and D.

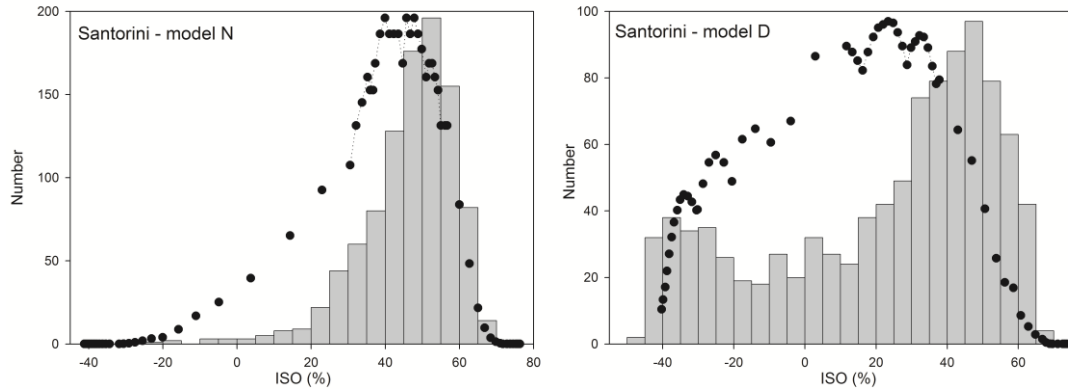


Figure 3.3. The uncertainty assessment of the isotropic component, calculated using equations (5-7) from Vackář et al. (2017) in two crustal models, N and D compared with results of $\text{pdf}(a_6)$, calculated using equation (3.9).

Santorini island - weaker event - results

The results for pdf function calculations according to eq. (3.9) are shown in the Figure 3.4. We can see that in this case the ISO component is smaller than for the strongest event of Santorini earthquake swarm. For the model D we cannot distinguish which value of ISO is correct.

Although we believe that both chosen earthquakes from Santorini earthquake swarm have positive isotropic component of MT, we get negative values of ISO for calculations in model D (ISO = -24%), accompanied with large values of CN (CN = 6). The similar conclusions about poor resolvability of ISO component in model D we can get from jackknife tests. In all results for model N the value of CN is less than 5.0. In the sense of CN, the results for full MT in model D are less stable than for full MT in model N. Therefore, the values of ISO are more trustable for model N than for model D. It seems that if CN is larger than 6 the value of ISO could be completely wrong (although strike, dip, rake values have reasonable values).

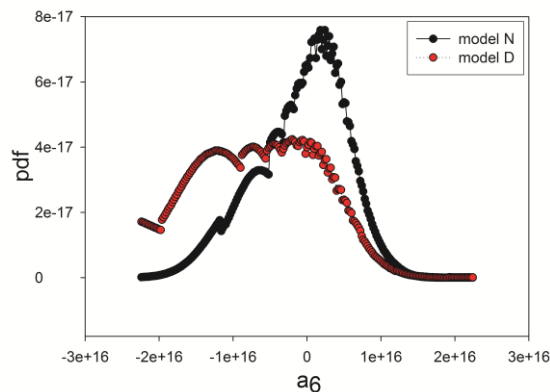


Figure 3.4. The uncertainty assessment of the isotropic component, $\text{pdf}(a_6)$, calculated using equation (3.9) in two crustal models, N and D for Santorini earthquake – second strongest event.

Cretan Sea earthquake - results

The results for pdf function calculations according to eq. (3.9) are shown in the Figure 3.5. We can see that this outcome is in good agreement with result obtained during full MT calculation where in this case the ISO component is negative and has

relatively small value ($ISO = -9.6\%$). The resolvability of ISO component according to Figure 3.5 is great. The similar conclusions about ISO we can get from jackknife tests. Probability of $a_6 = 0$ ($ISO = 0$) is high thus indicating that vanishing volume change for this event can be a reasonable interpretation.

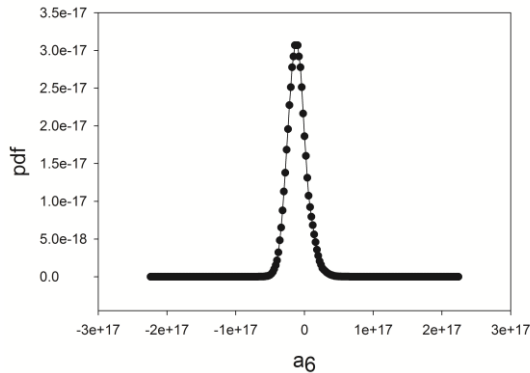


Figure 3.5. The uncertainty assessment of the isotropic component, $pdf(a_6)$, calculated using equation (3.9) for Cretan Sea earthquake.

Synthetic tests - results

In most sub-tests of Test A, the strike/dip/rake angles of the deviatoric inversion differ only marginally from the correct solution. However, there are two exceptions, corresponding to the MT with the largest ISO $\pm 89.5\%$. For these cases, the deviatoric inversion produces a MT whose CLVD is greater than 90%, and the fault-plane solution of the deviatoric inversion differs quite significantly from the correct one. However, nodal lines on beach balls make very limited sense if the ISO component of MT is (in absolute value) close to 90% or higher.

The sub-tests of Test B, representing similar experiment but with different strike/dip/rake angles and a slightly shallower depth, give almost the same results. For details see Tables A3-A5 in Křížová et al. (2016).

In Test C, where the inversion is performed for the incorrect velocity model, we obtain deviations from the correct solution even in the full-MT inversion. The prescribed (correct) values are those of test B, due to the incorrect velocity model, in this case C. The latter is the case of sub-tests C1D and C2D, with “real” $ISO = -90.3\%$ and $+90.4\%$ where we obtain only $ISO = -70.1$ and $+75.1$, respectively. For sub-test C2D-full we get Kagan angle as large as 91° . For two smaller (absolute) values of ISO, the full MT inversion gives a higher VR and small K-angle. The deviatoric inversion in the incorrect model provides relatively small deviation of the nodal lines from the correct solution. It means that, in this example, the inversion of the fault plane solution is robust. For the deviatoric inversion, the DC% is almost always biased, for the low input DC% (sub-test 1, also accompanied by a very wrong retrieved depth). However, for the full inversion the retrieved DC% is relatively close to the true one (or somewhat lower). The DC% for the full MT inversion is retrieved well in case 1 and 2, but in tests 3-6 it is lower than the true value. Our results show that an incorrect velocity model introduces bias in estimating the DC% in both the full and deviatoric inversions.

We should mention that we generate synthetic data without noise and then invert them, that is why the results for full MT inversion in model N are considered to be correct.

We inverted the synthetic data in full-MT mode and no pronounced local maxima can be detected. In other words, for this particular event-station geometry and velocity model, the centroid depth resolvability is almost none. The (weak) depth variation is almost independent on ISO%. There is a weak dependence on depth for sub-tests 3-6, but the shape of curves is almost the same. The correlation seems to be least dependent on depth in subtests 1 and 2, the curves are almost flat.

The inversion of the same synthetic data in deviatoric mode clearly shows that neglecting the isotropic component has a strong effect upon the correlation-depth variations. In particular, sub-tests 1 and 2 show very deep local minima, but weaker local minima can be observed also in the other sub-tests. The minima are close (but not identical) to the true source depth. This remarkable feature is common to all tests A-C. The tests indicate that if a real event has a very large ISO% (low DC%), the correlation-depth graph may get an apparent minimum near the correct source depth, i.e. the depth will be incorrectly determined.

3.3. Summary of Chapter 3

The three earthquakes were investigated: two strongest event of Santorini Island earthquake swarm and strongest event of Cretan Sea earthquake swarm. Group of synthetic tests with same station source distribution like in real case for two of chosen earthquakes was performed.

To more deeply investigate possible non-DC components, we study the depth-dependent correlation in two modes – full and deviatoric. For Cretan sea earthquake, our CLVD value (~6%) is smaller than the CLVD value (43%) obtained in previous modeling, using a different code and station geometry (Kiratzi, 2013). For Santorini earthquake – strongest event, we expect a large ISO component because standard deviatoric centroid MT inversion indicated the double-couple percentage as low as 59%. Two velocity models for Santorini earthquake were used (D-model and N-model).

The two events studied in Křížová et al. (2016) are very different. The Cretan Sea has a large DC% for both inversion modes in a broad range of the trial source depths, and the correlation-depth variations are almost identical. These are indications of a low ISO component. Contrarily, the Santorini Island earthquake (strongest event of swarm) has a lower DC% at the depths where the correlation takes its maximum values. Most importantly, the full-MT and deviatoric-MT inversions provide considerably different correlation-depth dependences. Compared to the synthetic tests we interpret these features as an indicator for a large isotropic component of the Santorini Island event. On the other hand, the missing local minimum in correlation function for Cretan Sea earthquake indicates relatively low ISO component.

The detailed synthetic tests have some practical implications. We think that the message of the synthetic tests is quite strong. They suggest that if the data processing indicates a small DC%, the correlation-depth analysis should be made twice, both in the full-MT and deviatoric-MT mode. If these two results strongly differ from each other, they may indicate the presence of a large isotropic component.

As an earthquake with possible large isotropic component of MT the strongest event from the Santorini Island earthquake swarm was studied. This event has relatively large ISO in model N in jackknife tests. Although results for model D have higher values of variance reduction (eq. 1.19) we accepted more the outcomes for model N because of smaller value of CN (eq. 3.1), this is especially true for ISO component of MT.

Conclusions

While the centroid moment tensor (CMT) calculations belong to routine seismological tasks, the uncertainty estimate of CMT is still rather a research problem, particularly regarding the isotropic component.

Therefore, new and robust techniques applicable in seismological practice are necessary, particularly in volcano seismology, in studies of geothermal regions, or in nuclear-test monitoring, where the isotropic component may be significant.

Two new approaches to assess resolvability of isotropic component of CMT were proposed in this thesis. The main results were published in two papers, Křížová et al. (2013; 2016), and are briefly summarized below. The approaches were validated on synthetic tests and real data. For testing the methods, three shallow earthquakes from Greece were chosen: The Cretan Sea, M_w 5.3 event of 27 January 2012, the Santorini M_w 4.9 event of 26 June 2009, and the Santorini M_w 4.7 event of 26 June 2009. We focused on the use of near-regional, low-frequency broad band waveforms.

First approach

In linearized inversion problems, where the earthquake or explosive-source location and origin time are fixed (e.g. assumed to be known), the uncertainty of the moment tensor can be studied through the eigenvalues and eigenvectors of the design matrix, which allows the representation of the theoretical misfit by means of a 6D error ellipsoid. Because the design matrix depends only on the structural model and receiver source geometry, the analysis can be performed using recorded seismic waveforms, or even without. In the non-linear inversion problems, where the free parameters are eight (e.g., the six elements of the moment tensor, depth, and origin time), we propose a waveform-inversion scheme in which the moment-tensor trace is systematically varied, and the remaining seven free parameters are optimized for each specific value of the trace. In this way, the waveform misfit can be studied as a function of the moment tensor, centroid depth, and centroid time. In particular, misfit

as a function of the moment-tensor trace enables a relative comparison of events as regards their isotropic component. To account for uncertain crustal structure the method is applied in this thesis repeatedly in two velocity models available in the studied region.

Applying this method to the two shallow earthquakes (M_w 4.9 and 4.7) with epicenters close to the Columbo volcano, located 20 km northeast of the island of Santorini, Aegean Sea, Greece we found that a notable feature is the strong trade-off between the isotropic component and source depth. It is stronger than the trade-off of the isotropic component with the seismic moment, source angles (strike, dip, and rake) and origin time. Very prominent is the effect of the crustal models used: model N (Novotný et al., 2001) and model D (Dimitriadis et al., 2010). Both structural models provide satisfactory waveform match of observed and synthetic seismograms, however, if the true structure of the Earth is closer to model D, then the isotropic component is almost irresolvable. From these two existing velocity models, we prefer the model N with lower condition number, in which a large positive isotropic component is indicated for strongest event of Santorini Island earthquake swarm.

Second approach

We formulated and partly verified a hypothesis that events with a significant isotropic component can be detected by a simple comparison of the full-MT and deviatoric-MT inversions, and that the centroid depth determination of such events under deviatoric constraint may be highly inaccurate.

Current MT determinations are often made in deviatoric approximation, and they include a grid search of the centroid position and time. The centroid is identified with a trial source position that maximizes correlation between real and synthetic waveforms. We proposed that the waveform inversion should be made in two modes: the full MT and the deviatoric MT. If the two inversion modes provide remarkably different correlation-depth functions and, in particular, if the correlation of the deviatoric inversion possess a deep local minimum (although in the full-MT inversion such a minimum is absent), we obtain an indication of a strong isotropic component. The likely source depth is close to that local minimum. Because in routine practice just the maximum of the correlation-depth function provides an estimate of the centroid depth, we infer that in case of the deviatoric inversion of an event with large ISO this traditional approach may fail, returning an incorrect depth (and possibly also an incorrect fault-plane solution).

Interestingly, synthetic tests indicating the mentioned features of the correlation-depth functions are quite robust. Indeed, the characteristic features were found even in the case when synthetic waveforms simulated in one velocity model were inverted in another model available for the same region.

Applying this method to the two studied earthquakes we found that for the Santorini Island earthquake (strongest event of swarm) the full-MT and deviatoric-MT inversions provide considerably different correlation-depth dependences. Based on the synthetic tests we interpret these features as an indicator for a large isotropic

component of the Santorini Island event. On the other hand, the missing local minimum in correlation function for Cretan Sea earthquake indicates relatively low ISO component.

In this sense, the second approach provided an independent confirmation of a significant isotropic component of strongest event of Santorini Island earthquake swarm, previously indicated from the first approach.

Final remark

Both the proposed approaches are comprehensible and they are usable in practice. Use of the first approach would be facilitated by its inclusion in ISOLA released software package. Use of the second approach is quite straightforward. Real usefulness of the developed methods should be tested in future on more earthquakes, in particular on such events for which uncertainty estimates of the isotropic component by independent techniques would be available.

Bibliography

- Aki, K., and P. G. Richards (2002), *Quantitative seismology*, University Science Books, Sausalito, California, 704 pp.
- Bouchon, M. (1981). A simple method to calculate Green's functions for elastic layered media, *Bull. Seismol. Soc. Am.* **71**, 959-971.
- Cesca S, S. Heimann, K. Stammer, T. Dahm (2010). Automated procedure for point and kinematic source inversion at regional distances. *J. Geophys. Res.* **115**:B06304. doi:10.1029/2009JB006450
- Chapman, C. H., and W. S. Leaney (2012). A new moment-tensor decomposition for seismic events in anisotropic media, *Geophys. J. Int.*, **188**, 343–370.
- Coutant, O. (1989). Program of numerical simulation AXITRA, *Tech. rep.*, LGIT, Grenoble, France (in French).
- Dahlen, F. A., and J. Tromp (September 1998). Theoretical Global Seismology.
- Dimitriadis, I., C. Papazachos, D. Panagiotopoulos, P. Hatzidimitriou, M. Bohnhoff, M. Rische, and T. Meier (2010). P and S velocity structures of the Santorini-Coloumbo volcanics system (Aegean Sea, Greece) obtained by non-linear inversion of travel times and its tectonic implications, *J. Volcanol. Geoth. Res.* **195**, 13-30.
- Dreger, D. S. (2002). Time-Domain Moment Tensor INVerse Code (TDMT-INVC); Chapter 85.11 of the IASPEI International Handbook of Earthquake and Engineering Seismology (ftp://www.orfeus-eu.org/pub/software/iaspei2003/8511_tutorial.pdf - last accessed May 2017)
- Dreger, D. S., H. Tkalčić, and M. Johnston (2000). Dilational processes accompanying earthquakes in the Long Valley caldera. *Science* **288**, 122 (2000), DOI: 10.1126/science.288.5463.122.
- Gallovič, F., J. Zahradník, D. Křížová, V. Plicka, E. Sokos, A. Serpetsidaki, and G-A. Tselentis (2009). From earthquake centroid to spatial-temporal rupture evolution: Mw 6.3 Movri Mountain earthquake, June 8, 2008, Greece, *Geophys. Res. Let.* **36**, L21310, doi: 10.1029/2009GL040283.

- Green, G. (1828). An essay on the application of mathematical analysis to the theories of electricity and magnetism. Nottingham [Eng.: Printed for the author, by T. Wheelhouse].
- Haslinger, F., E. Kissling, J. Ansorge, D. Hatzfeld, E. Papadimitriou, V. Karakostas, K. Makropoulos, H.-G. Kahle, and Y. Peter (1999). 3D crustal structure from local earthquake tomography around the Gulf of Arta (Ionian region, NW Greece). *Tectonophysics*, **304**(3), 201-218.
- Heimann, S. (2010). A robust method to estimate kinematic earthquake source parameters. PhD Thesis, University of Hamburg, Germany, pp 145
- Hicks, S. P., and A. Rietbrock (2015). Seismic slip on an upper-plate normal fault during a large subduction megathrust rupture. *Nature Geoscience*, **8**(12), 955-960, doi:10.1038/ngeo2585.
- Jechumtálová, Z., J. Šílený (1998). Smoothing the source time function – a tool to soften inadequate modelling of the medium during inversion of local waveforms? *Journal of Seismology*, **2**, 145-158.
- Jechumtálová, Z., J. Šílený (2001). Point-source Parameters from Noisy Waveforms: Error Estimate by Monte-Carlo Simulation. *Pure Appl. Geophys.* **158**, 1639-1654.
- Jost, M. L., and R. B. Herrmann (1989). A students guide to and review of moment tensors, *Seismol. Res. Lett.* **60**, 37–57.
- Julian, B. R., A. D. Miller, and G. R. Foulger (1998). Non-double-couple Earthquakes, 1, *Rev. Geophys.* **36**, 525-549.
- Kagan, Y. Y. (1991). 3-D rotation of double-couple earthquake sources, *Geophys. J. Int.* **106**, 709-716, doi 10.1111/j.1365-246X.1991.tb06343.x.
- Karagianni, E. E., C. B. Papazachos, D. G. Panagiotopoulos, P. Suhadolc, A. Vuan, and G. F. Panza (2005). Shear velocity structure in the Aegean area obtained by inversion of Rayleigh waves. *Geophys. J. Int.*, **160**(1), 127-143.
- Kikuchi, M., and H. Kanamori (1991). Inversion of complex body waves. III, *Bull. Seismol. Soc. Am.* **81**, 2335–2350.
- Kiratzí, A. (2013). The January 2012 earthquake sequence in the Cretan Basin, south of the Hellenic Volcanic Arc: Focal mechanisms, rupture directivity and slip models, *Tectonophysics*, **586**, 160-172, doi: 10.1016/j.tecto.2012.11.019.
- Křížová, D., J. Zahradník, and A. Kiratzí (2013). Resolvability of Isotropic Component in Regional Seismic Moment Tensor, Inversion, *Bull. Seismol. Soc. Am.* **103**, no. 4, 2460 - 2473, doi: 10.1785/0120120097.
- Křížová, D., J. Zahradník, and A. Kiratzí (2016). Possible Indicator of a Strong Isotropic Earthquake Component: Example of Two Shallow Earthquakes in Greece, *Bull. Seismol. Soc. Am.* **106**, no. 6, 2784 - 2795, doi: 10.1785/0120160086.
- Latorre, D., J. Virieux, T. Monfret, V. Monteiller, T. Vanorio, J. L. Got, and H. Lyon-Caen (2004). A new seismic tomography of Aigion area (Gulf of Corinth, Greece) from the 1991 data set. *Geophys. J. Int.* **159**(3), 1013-1031.
- Lay, T. , T. C. Wallace (1995), Modern global seismology. Academic Press 1995.
- Novotný, O., J. Zahradník, and G-A. Tselentis (2001). Northwestern Turkey earthquakes and the crustal structure inferred from surface waves observed in Western Greece, *Bull. Seismol. Soc. Am.* **91**, 875-879.
- Pasyanos, M., D. S. Dreger, and B. Romanowicz (1996). Towards real-time determination of regional moment tensors. *Bull. Seismol. Soc. Am.* **86**, 1255–1269.

- Press, W. H., S. A. Teukolsky, W. T. Vetterling, and B. P. Flannery (1997). *Numerical recipes in Fortran 77: The art of Scientific Computing*, Cambridge University Press, 2nd ed., 992 pp.
- Richter, C. F. (1935). An instrumental earthquake magnitude scale. *Bull. Seismol. Soc. Am.* **25** (1–2): 1–32.
- Rigo, A., H. Lyon-Caen, R. Armijo, A. Deschamps, D. Hatzfeld, K. Makropoulos, P. Papadimitriou, and I. Kassaras (1996). A microseismic study in the western part of the Gulf of Corinth (Greece): Implications for large-scale normal faulting mechanisms. *Geophys. J. Int.* **126**(3), 663–688.
- Silver, P. G., and T. H. Jordan (1982). Optimal estimation of scalar seismic moment, *Geophys. J. Roy. Astron. Soc.* **70**, 755–787, doi: 10.1111/j.1365-246X.1982.tb05982.x.
- Sokos, E. N., and J. Zahradník (2008). ISOLA a Fortran code and a Matlab GUI to perform multiple-point source inversion of seismic data. *Comput. Geosci.* **34**, 967–977.
- Sokos, E. and J. Zahradník (2013). Evaluating centroid moment tensor uncertainty in new version of ISOLA software, *Seismol. Res. Lett.* **84**, 656–665.
- Tarantola, A. (2005). Inverse Problem Theory and Methods for Model Parameter Estimation. Institut de Physique du Globe de Paris, Université de Paris 6, Paris, France. DOI: <http://dx.doi.org/10.1137/1.9780898717921>
- Tselentis, G.-A., N.S. Melis, E. Sokos, and K. Papatsimpa (1996). The Egion June 15, 1995 (6.2 ML) earthquake, Western Greece. *Pure Appl. Geophys.* **147**, 83–98.
- Vackář, J., J. Burjánek, F. Gallovič, J. Zahradník, and J. Clinton (2017). Bayesian ISOLA: new tool for automated centroid moment tensor inversion. *Geophys. J. Int.* doi: <https://doi.org/10.1093/gji/ggx158>
- Vavryčuk, V. (2001). Inversion for parameters of tensile earthquakes, *J. Geophys. Res.* **106**, 16,339–16,355.
- Zahradník, J., and S. Custódio (2012). Moment tensor resolvability: Application to southwest Iberia. *Bull. Seismol. Soc. Am.* **102**, 1235–1254, doi: 10.1785/0120110216.

Web pages:

- www.emsc-csem.org/ - last accessed May 2017 (European-Mediterranean Seismological Centre (EMSC))
- <http://www.orfeus-eu.org/> - last accessed May 2017 (Observatories & Research Facilities for European Seismology = Orfeus)
- http://www.giseis.alaska.edu/input/carl/research/beach/beachnotes_percent.pdf - last accessed May 2017 (Tape, C. (2016). "Percentages" of DC, CLVD, ISO for moment tensors should be dropped)

List of author's publications and citation report

- ❖ Křížová, D., J. Zahradník, and A. Kiratzi (2016). Possible Indicator of a Strong Isotropic Earthquake Component: Example of Two Shallow Earthquakes in Greece, *Bull. Seismol. Soc. Am.* **106**, no. 6, 2784 - 2795, doi: 10.1785/0120160086.
 - Without citation (till 9th June 2017)

- ❖ Křížová, D., J. Zahradník, and A. Kiratzi (2013). Resolvability of Isotropic Component in Regional Seismic Moment Tensor, Inversion, *Bull. Seismol. Soc. Am.* **103**, no. 4, 2460 - 2473, doi: 10.1785/0120120097.
 - 14 citations (till 9th June 2017)

- ❖ Gallovič, F., J. Zahradník, D. Křížová, V. Plicka, E. Sokos, A. Serpetsidaki, and G-A. Tselentis (2009). From earthquake centroid to spatial-temporal rupture evolution: Mw 6.3 Movri Mountain earthquake, June 8, 2008, Greece, *Geophys. Res. Let.* **36**, L21310, doi: 10.1029/2009GL040283.
 - 22 citations (till 9th June 2017)